

Soft x-ray photoabsorption spectra of photoionized CH₄ and CO₂ plasmas

Lazaros Varvarezos¹, Hu Lu¹, John T Costello¹, Andrzej Bartnik², Przemysław Wachulak², Tomasz Fok², Łukasz Węgrzyński² and Henryk Fiedorowicz²

¹Dublin City University, School of Physical Sciences and NCPST, Dublin 9, Ireland

²Institute of Optoelectronics, Military University of Technology, Kaliskiego 2, 00-908 Warsaw, Poland

E-mail: lazaros.varvarezos2@mail.dcu.ie

Received 15 August 2019, revised 13 November 2019

Accepted for publication 3 December 2019

Published 27 January 2020



CrossMark

Abstract

In this work we report soft x-ray (SXR) photoabsorption measurements in neutral methane and carbon dioxide molecules and their corresponding photoionized plasmas. The SXR radiation was generated by a table-top laser produced plasma source based on a double stream gas puff target. At low SXR intensities only features related to neutral molecules are present in the absorption spectrum. On the other hand, as the radiation intensity increases, we observe new absorption features in the low photon energy side of the spectrum. In that case fragments such as neutral and ionized molecules, atoms and atomic ions are found to contribute to the absorption spectrum of the plasmas. To our knowledge these are the first measurements where this laser plasma based SXR source is used to both create and probe a molecular plasma. Emphasis is placed on identifying the fragment species and the corresponding transitions.

Keywords: soft x-rays, photoionized plasmas, soft x-ray spectroscopy

(Some figures may appear in colour only in the online journal)

1. Introduction

The water window region extends from the carbon K-shell absorption edge (284.2 eV) to the oxygen K-shell absorption edge (543.1 eV) and is particularly important for investigation of biological processes. In this spectral region, carbon, oxygen and nitrogen in cell tissues exhibit strong absorption whereas the neighboring water environment is transparent allowing for high-contrast biological imaging. To date, large scale facilities such as third generation synchrotrons or free electron lasers have been the primary sources of soft x-ray (SXR) radiation, however having the drawback of limited accessibility for external users. Emission of radiation in the water-window region can be produced by table-top sources based on the high harmonic generation process [1, 2] at the expense of conversion efficiency. Following a different approach, SXR radiation was generated in laser produced plasma (LPP) sources. The scheme implemented in our experiment was based on focusing the output of a Q-switched Nd:YAG laser into a double stream gas puff target, serving as

an active medium for generation of radiation in the water-window region [3].

Several previous studies have demonstrated the feasibility of creating and/or probing low temperature photoionized plasmas with XUV and SXR radiation from gas puff based LPP sources. Emission studies in the range of 10–20 nm were performed in Ne [4], irradiated by EUV photons (centered around 11 nm) generated by the Kr/Xe double gas puff target. The same experiment was performed using the Xe/Ne double gas puff target to record emission spectra of Ne in the UV/VIS region [5]. Similar spectroscopic investigations were conducted in He [6] and Kr [7], where emission spectroscopy was complemented by absorption measurements. The aforementioned studies were expanded to include molecular plasmas N₂ [8] and SF₆ [9] for which emission spectra were recorded in the VUV and UV/VIS range. In addition, temporal measurements of the emission from ionic atomic and molecular species were reported [10].

Absorption of a SXR photon can effectively remove one (or more) core and/or inner-shell electrons in neutral

molecules. Upon inner-shell photoionization the molecule relaxes via emission of an Auger electron or emission of an x-ray photon that could in turn induce further ionization of adjacent species. Alternatively, the core-excited molecular ion may dissociate into molecular and/or atomic ions residing in their ground or excited states. Since ions constitute the majority of matter in universe, photoionization is key to understanding gas-phase chemistry in extraterrestrial space [11]. Thus acquisition of spectroscopic data in atomic and molecular ions is still an ongoing challenge for researchers (see for example [12]).

From an experimentalist's standpoint, photoabsorption studies in atomic ions have been performed in synchrotrons using the merged beam technique [13]. In this arrangement monochromatized synchrotron radiation is merged with ions produced by a surface ionization source. This experimental approach has been widely applied in facilities such as Daresbury (UK) [14] and the Photon Factory [15] in Japan. These seminal experiments, suffered from weak signal rates due to the low density of ionic species. The advent of second generation light sources paved the way for permanent incorporation of merged beam setups at endstations in several facilities such as ALS [16], SOLEIL [17] and PETRA III [18].

Analogous photoabsorption studies in ionic species have been conducted by means of the dual laser plasma (DLP) technique [19]. In that case, the backlighting source is plasma emission, generated when high power laser pulses are focused onto solid targets. Pioneering work [20] carried out by Carillon and coworkers reported XUV absorption measurements in Al, using the DLP technique. The development of a DLP source covering the 1–10 Å spectral range, allowed for an absorption study in Al K-shell [21]. DLP has been proven a very useful tool for investigation of atomic ions [22], however DLP measurements in molecular species are rare in the literature. As high-temperature plasmas are generated in the DLP technique, electron collisions open dissociation pathways other than those induced by photodissociation hence adding complexity and ambiguity in the recorded spectra. In addition, molecular ions in excited states are expected to deexcite after the photodissociation of the parent molecule, long before the arrival of the time-delayed backlighting radiation. Thus photoabsorption studies of molecular ions in excited states seem challenging for the DLP scheme. Both the aforementioned difficulties are not present in the double gas puff target technique used here.

Low temperature photoionized plasmas constitute a very unique state of matter. Neutral atoms and molecules, radicals, ions and electrons are present when radiation in the SXR region is focused onto a dense gas medium. Contrary to the case of plasma formation directly by the optical laser, the SXR photon energy is high enough to ensure the release of core and valence electrons. Consequently, lower intensities are required for plasma creation, resulting in thermal electron temperatures on the order of 1–2 eV [9]. The domain of low temperature plasmas is particularly interdisciplinary and brings together several different research fields, extending from atomic and molecular physics, material and surface science, chemistry, to even biology and medicine (see review

[23]). From a different standpoint, photoionized plasmas are commonly encountered in astrophysics (see for example [24]). A typical example concerns plasmas generated in irradiated accretion disks around compact astrophysical objects such as neutron stars, black holes, or white dwarfs.

In this work, we report SXR absorption measurements of CH₄ and CO₂ photoionized plasmas. Emphasis here is on methane and carbon dioxide since, carbon dioxide is a major constituent of the terrestrial group (Mercury, Venus, Earth and Mars) whose atmospheric composition is by its very nature oxidizing (CO₂, O₂) whereas methane is abundant in the Jovian group (Jupiter, Saturn, Uranus and Neptune) whose atmospheric composition is reducing (H₂, CH₄, NH₃). Dissociation of the two molecules, produces ionic fragments such as CH₃⁺ and C⁺ which play a major role in astrophysical photochemistry. The former is effectively a source for more complex hydrocarbons via chemical interactions with methane or acetylene in the Jovian atmosphere. This way, it is possible to produce hydrocarbon ions consisting of more than two or three carbon atoms respectively. These ions then undergo dissociative recombination to form neutral hydrocarbons. The latter, is one of the most commonly encountered cometary ions. A DLP study has been carried out on carbon K-edge absorption in C²⁺, C³⁺, C⁴⁺ ions [25]. However, mixing between the different charge states was apparent in the photoabsorption spectra. Hence, an experimental study on C⁺ species without the simultaneous presence of multiple charge states is pursued in order to complement a previous study [26] based on the merged beams technique.

2. Experimental details

A schematic diagram of the experimental setup is shown in figure 1(a) and some photographs of the setup in figure 1(b). The laser beam was produced by a commercial table top NL129 (EKSPLA) Nd:YAG laser system emitting radiation at 1064 nm operating at a repetition rate of 10 Hz. The pulse energy was measured to be ≈ 6.7 J and the pulse duration was measured by means of a photodiode to be ≈ 1.6 ns. The laser beam was focused, using a 10 cm focal length lens, into a double stream gas puff target in order to generate the plasma. This gas puff target consists of two concentric nozzles: the inner nozzle has a diameter of ≈ 0.4 mm and the outer nozzle is ring-shaped with a diameter of ≈ 0.7 –1.5 mm. The two nozzles are driven independently by two electromagnetic actuators. In this geometry, a low Z gas is used to confine a high Z gas. In our experiment we used two different inner gases, Kr and a mixture of Kr/Xe (90/10), while maintaining He as the outer gas. By using the double gas puff target, a conversion efficiency as high as $\sim 0.42\%$ has been achieved for a wavelength of 13.5 nm [27], using a Xe/He target. The molecular gases to be irradiated by the SXR radiation from the double gas puff plasma source, are then injected into the vicinity of the LPP source by means of an additional valve ≈ 2 mm in diameter. Differential pumping was applied to evacuate the two parts of the chamber leading to a base pressure of $\approx 10^{-4}$ mbar. The radiation emitted by the LPP source can then serve a two-fold role: first, it photoionizes the molecular gases to form the

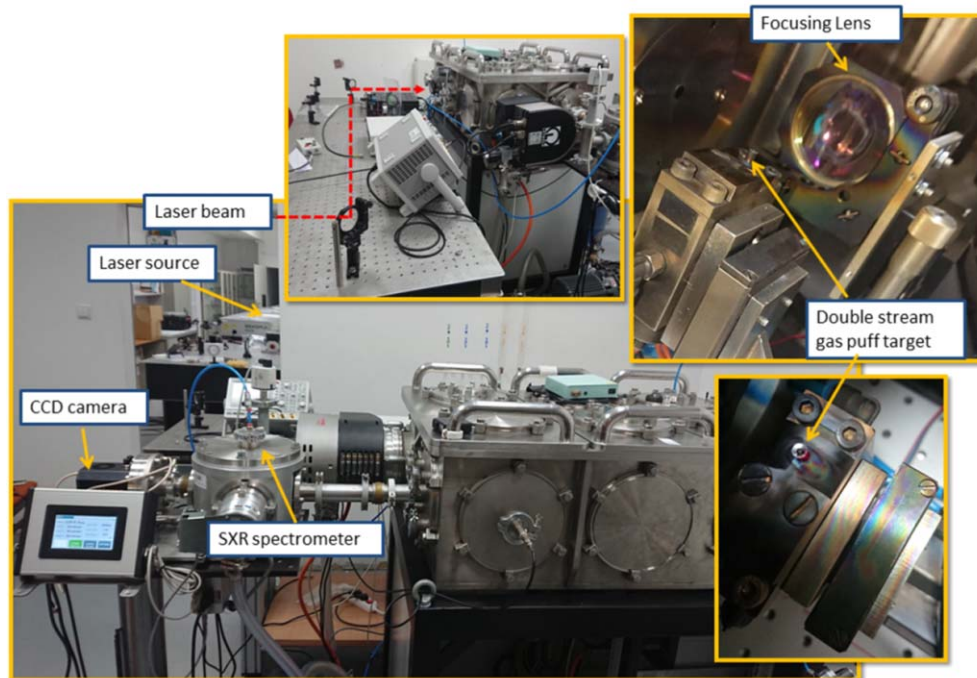
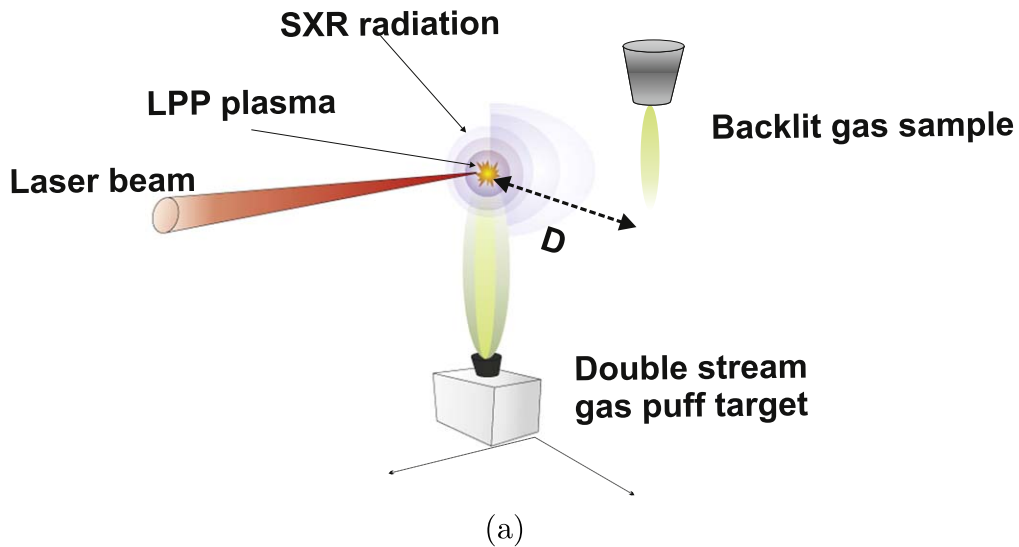


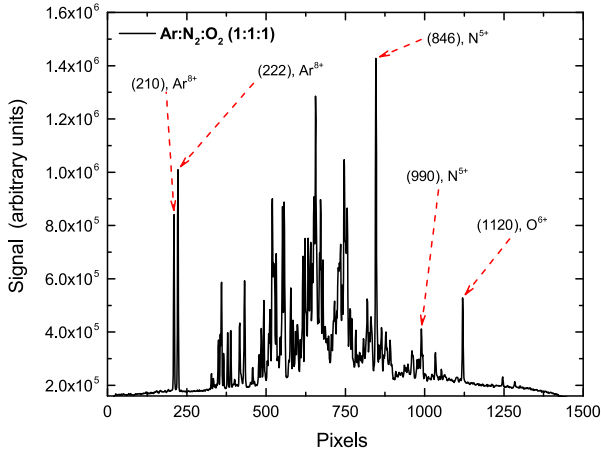
Figure 1. (a) Schematic diagram of the setup. The laser beam is focused onto the double stream gas puff target to generate soft x-ray radiation. The emitted radiation is then used to perform absorption measurements on a molecular gas target located at a distance (D) away from the source. (b) Photographs of the experimental setup.

Table 1. Tabulated optimum experimental parameters.

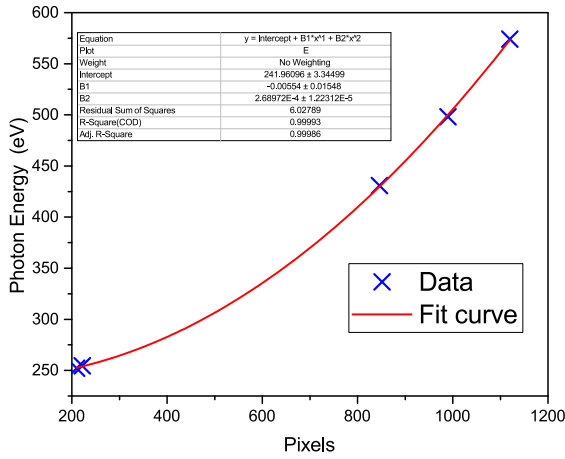
Gas species	T_{Delay} (μs)	Operating backing pressure (bars)
Kr	750	9
Kr/Xe	700	9
CO ₂	500	4
CH ₄	800	1
He	700	6

plasmas and secondly, the continuous part of the radiation acts as a SXR backlight for the photoionized plasmas. This arrangement allows for one photon absorption measurements of the photoionized molecular plasmas.

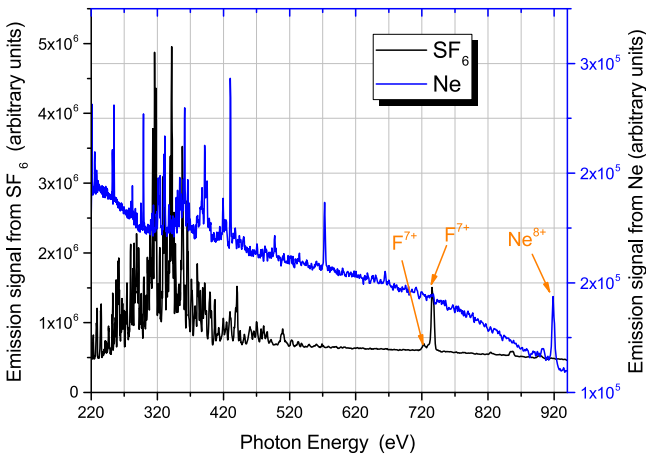
The absorption spectra were recorded via a home-made spectrograph with a grazing incidence diffraction grating (Hitachi High Technologies America Inc., Baltimore, MD, USA) [28, 29] with 2400 lines per mm, and a wavelength range extending from 1 to 5 nm. For the detection of the



(a)



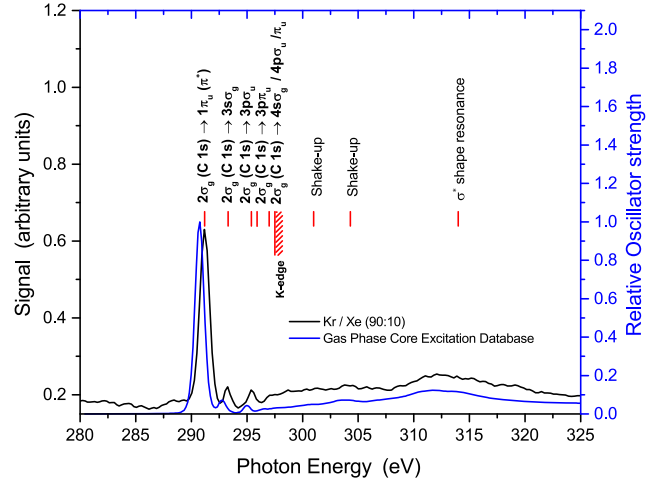
(b)



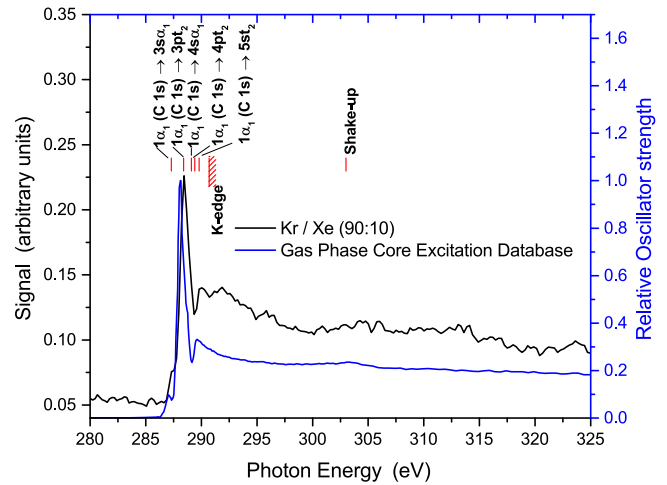
(c)

Figure 2. (a) Soft x-ray emission spectrum of the $N_2:O_2:Ar$ (1:1:1) gas mixture. (b) The calibration curve of the spectrometer. (c) Soft x-ray emission spectrum of SF_6 and Ne.

spectra a back-illuminated CCD camera (Greateyes GmbH, Berlin, Germany) was placed after the diffraction grating. The camera has a chip with 2052×2046 pixels, the size of which was $13 \times 13 \mu m^2$. Throughout the experimental process, the chip was cooled down to $-40^\circ C$ to reduce its internal noise and background.



(a)



(b)

Figure 3. Experimental SXR absorption of the ‘not ionized’ (a) carbon dioxide and (b) methane plotted together with the normalized oscillator strength adapted from [33]. A gas mixture of xenon/krypton (90/10) was used as the medium to generate the soft x-ray backlighting radiation.

In order to enhance the SXR emission, we optimized the performance of our source by varying several parameters. Firstly we arranged for the gas puff target to be triggered before the arrival of the laser pulse. Two parameters were tweaked for each valve, the first one was the delay time with respect to the instant of arrival of the valve trigger pulse and the second was the duration of the valve opening. In our case the duration of the valve opening was set at its maximum value as ($D = 1 \text{ ms} - T_{\text{Delay}}$). Hence the delay times were optimized for both the inner and the outer gases of the double stream gas puff target. In addition the optimum operating pressures were determined by previous experience. More information regarding the timing and synchronization can be found in [30, 31]. The optimum parameters for each gas are tabulated in table 1.

Moving to the next step, we performed a calibration of the SXR spectrometer. To do so, we used the emission spectrum of a gas mixture composed of $N_2:O_2:Ar$ (1:1:1) to

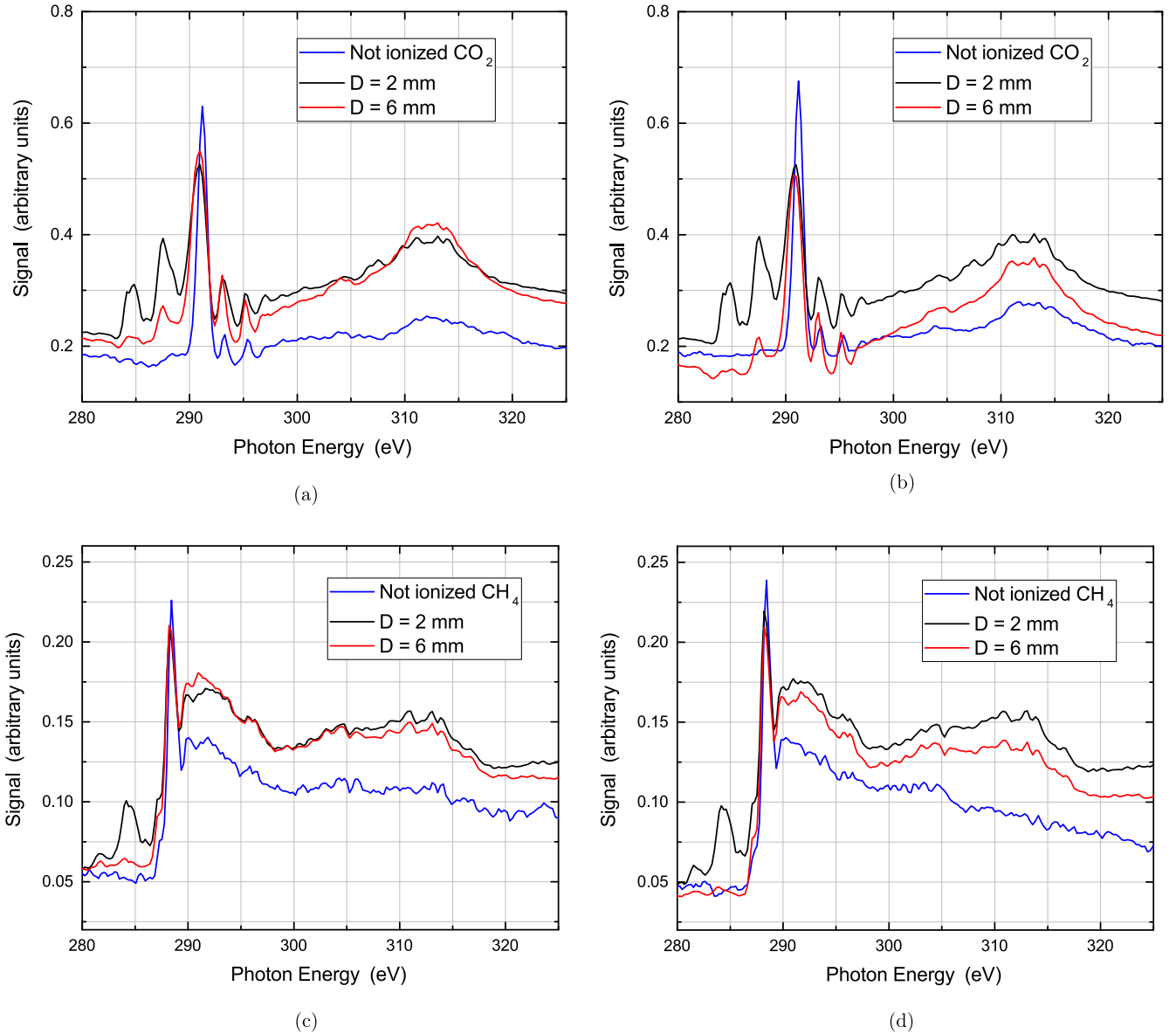


Figure 4. Absorption measurements around Carbon K-edge in CO₂ for three distances with respect to the LPP Soft x-ray source (a) using the Kr/Xe mixture and (b) using Kr in the double stream gas puff SXR source. Corresponding spectra for methane (c) using the Kr/Xe mixture as the inner gas and (d) using Kr as the inner gas, in the double stream gas puff SXR source.

identify several emission lines as seen in figure 2(a). Hence, we identified several lines associated with atomic ions present in the molecular plasma [32]. Specifically, for Ar⁸⁺ two lines were identified at 252.1 eV and at 254.5 eV, for N⁵⁺ two lines at 430.9 eV and 498.2 eV, and for O⁶⁺ one line at 574.0 eV. In order to calibrate the spectrometer, the data were fitted to a quadratic equation (see figure 2(b)), leading to the relationship below between the CCD pixel number and the corresponding photon energy (in eV):

$$y(x) = 2.69 \times 10^{-7}x^2 - 5.50 \times 10^{-3}x + 241.96, \quad (1)$$

where y is the photon energy in eV and x denotes the pixel index in the image recorded by the CCD camera. Then, we recorded the SXR emission spectra of Ne and SF₆, as presented in figure 2(c). From this spectrum, we identified two

emission lines for F⁷⁺ at 738.1 eV and at 723.0 eV, and a line of Ne⁸⁺ at 918.5 eV. The resolving power of the spectrometer, for a 12 μm slit was determined by the isolated line at 281.5 eV, associated with the $2s^22p^23d - 2s^22p^3$ transition of S⁹⁺ ions in the SF₆ plasma. The FWHM for this line was measured approximately 0.3 eV resulting in $E/\Delta E \simeq 900$.

3. Results and discussion

The SXR absorption measurements, were performed at two different distances, denoted as $D = 2$ mm and $D = 6$ mm, between the double stream gas puff target and the single stream gas puff target under investigation. In addition, the sample gas target was moved several tens of centimeters away

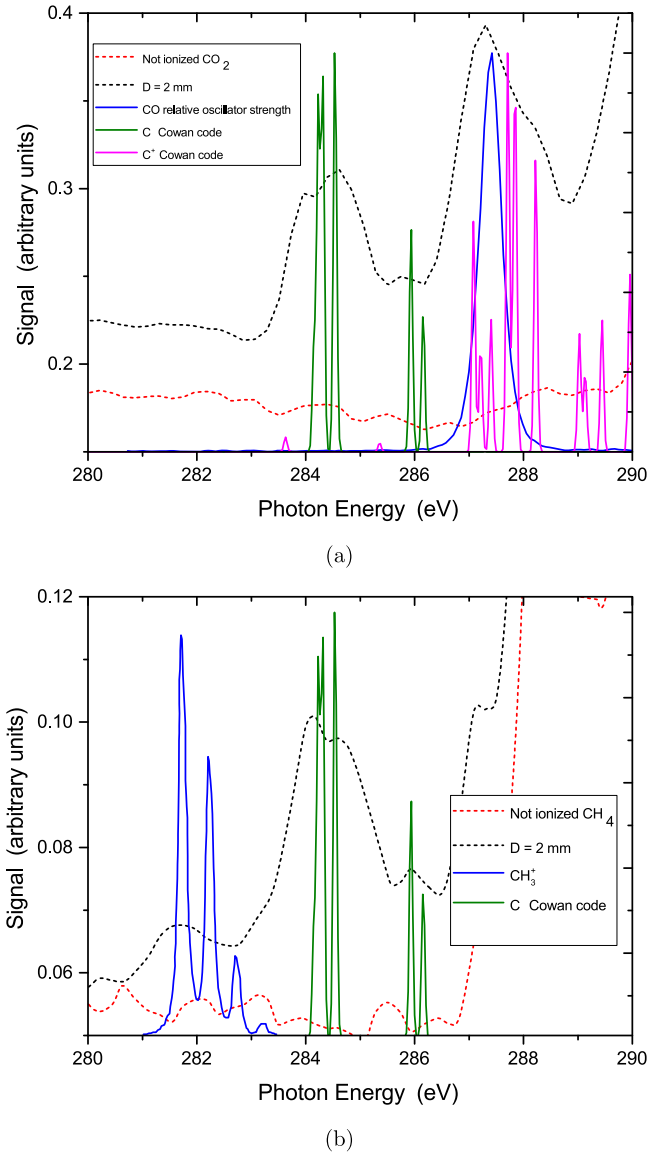


Figure 5. (a) The low-energy part of the Soft x-ray absorption spectrum of CO_2 plotted together with the normalized oscillator strength of CO [33], and calculations performed by means of the Cowan code for C and C^+ . (b) Similar spectrum for CH_4 plotted together with the calculated absorption spectrum of CH_3^+ [41], and calculations performed by means of the Cowan code [46, 47] for C and C^+ .

from the SXR source to record the absorption spectrum of the so called ‘not ionized’ sample. The measurements reported represent an average of 100 single shot spectra.

In figure 3(a) we present the SXR absorption spectrum of the carbon dioxide together with the relative oscillator strength of the same molecule obtained from the Gas Phase Core Excitation Database [33]. In that case the distance between the two valves was ≈ 35 cm, and one can see that the spectrum contains only features of the neutral ‘not ionized’ CO_2 molecule. From this spectrum, we were able to identify several absorption features in agreement with previously reported absorption measurements performed at synchrotron facilities [34–36].

Table 2. Tabulated transitions for the CO_2 and CH_4 plasmas, including transitions in CH_3^+ , CO, C, C^+ species.

Photon energy (eV)	Molecular/atomic species	Assignment
281.8	CH_3^+	$(1\alpha'_1)(C1s) \rightarrow (1\alpha'_2) (0 - 0)$
282.2	CH_3^+	$(1\alpha'_1)(C1s) \rightarrow (1\alpha'_2) (1 - 0)$
284.2	CI	$1s^2 2s^2 2p^2 (1S)^3P \rightarrow 1s^1 2s^2 2p^3 (4S)^3S$
284.3	CI	$1s^2 2s^2 2p^2 (1S)^3P \rightarrow 1s^1 2s^2 2p^3 (2D)^3D$
284.5	CI	$1s^2 2s^2 2p^2 (1S)^1D \rightarrow 1s^1 2s^2 2p^3 (2D)^1D$
285.9	CI	$1s^2 2s^2 2p^2 (1S)^3P \rightarrow 1s^1 2s^2 2p^3 (2P)^3P$
286.2	CI	$1s^2 2s^2 2p^2 (1S)^1D \rightarrow 1s^1 2s^2 2p^3 (2P)^1P$
287.1	CII	$1s^2 2s^1 2p^2 (4S)^4S \rightarrow 1s^1 2s^1 2p^3 (3P)^4P$
287.2	CII	$1s^2 2s^1 2p^2 (2P)^2P \rightarrow 1s^1 2s^1 2p^3 (1S)^2S$
287.4	CII	$1s^2 2s^1 2p^2 (2D)^2D \rightarrow 1s^1 2s^1 2p^3 (3P)^2P$
287.7	CII	$1s^2 2s^1 2p^2 (2D)^2D \rightarrow 1s^1 2s^1 2p^3 (1D)^2D$
287.8	CII	$1s^2 2s^2 2p^1 (1S)^2P \rightarrow 1s^1 2s^2 2p^2 (1D)^2D$
287.9	CII	$1s^2 2s^2 2p^1 (1S)^2P \rightarrow 1s^1 2s^2 2p^2 (3P)^2P$
288.2	CII	$1s^2 2s^1 2p^2 (2D)^2D \rightarrow 1s^1 2s^1 2p^3 (3P)^4P$
287.4	CO	$2\sigma(C1s) \rightarrow 1\pi_u, \pi \text{ resonance}$

Let us now turn our attention to the ‘not ionized’ CH_4 . Again, the absorption spectrum closely resembles the absorption of the neutral methane as shown in figure 3(b). Several absorption features were identified in accordance with the previously reported synchrotron studies [37–40]. The absorption spectra shown in figures 3(a) and (b) were performed using the krypton/xenon mixture as the medium to generate the SXR radiation. Similar measurements were recorded using krypton in the LPP source, in order to confirm the absence of artifacts in our spectrum stemming from the source itself.

In figures 4(a) and (c) absorption measurements are presented for CO_2 and CH_4 respectively using the Kr/Xe gas target SXR source. The spectra shown are for SXR source to sample distances ‘D’ of 2 mm, 6 mm and ≈ 350 mm. Several new features arise in the low energy region of the spectrum below the main absorption peak for both target molecules. This pattern is also present when Kr alone is applied as the inner gas for the SXR source as indicated by figures 4(b) and (d).

The additional features observed should be attributed to molecular and atomic species, produced by photochemical events taking place in the molecular plasma. In fact, the features in the SXR absorption spectrum of methane (figure 5(b)) can be attributed to the CH_3 radical and the C atom. Specifically, the CH_3 radical might account for the structure at ≈ 281 – 283 eV. This should involve an excitation from the core orbital to the outer valence orbital. As previously reported [41] this transition is associated with the so-called ‘umbrella motion’ of methyl radical. Similarly, absorption from atomic carbon could result in the features at ≈ 284 – 286 eV. The presence of the methyl radical is not surprising as the predominant dissociation pathway for methane is $\text{CH}_4 + h\nu \rightarrow \text{CH}_3^+ + \text{H}^+$ following a double ionization process in the SXR region where the photon energy

is high enough to remove two electrons from the valence orbital ($1t_2$). Neutral carbon can also be formed via a many-body fragmentation process of the methane dication (see [42]). In figure 5(a) we present the normalized oscillator strength of CO obtained from the Gas Phase Core Excitation Database [33], together with calculations performed by means of the Cowan code for the C atom and C^+ ion in the spectral region below 290 eV. As can be seen, the broad structure above ≈ 287 eV should be attributed to CO and C^+ whereas absorption from atomic carbon could result in the features at ≈ 284 – 286 eV. The presence of CO in the absorption spectrum, is a signature of the $CO_2^+ \rightarrow CO + O^+$ dissociation pathway following the removal of an inner valence $4\sigma_g$ electron [43]. Similar to the case of methane, the presence of C and C^+ should be attributed to many-body fragmentation processes. Such a pathway, has been observed when carbon dioxide was irradiated by synchrotron radiation, tuned to wavelengths around the oxygen or carbon K-edge [44]. In that case, a triple ionization followed by the $CO_2^{3+} \rightarrow C^+ + O^+ + O^+$ dissociation pathway, was suggested as the plausible explanation for the C^+ signal. In addition, a more recent study at the ALS supported the $CO_2^+ \rightarrow C^+ + O^+ + O$ pathway [45]. Undoubtedly, the most striking observation in our study, is the presence of states with an L-shell vacancy (core hole) in the C^+ ions. These states are then probed by a further photoabsorption step. The negligible time delay between the creation of the photoionized plasma and the absorption measurement along with the very short duration of the XUV pulse ensure that such states could only be created by photons from the laser plasma source and not particles which would reach the sample gas long after the XUV probe pulse has terminated. The aforementioned transitions, lying in the low energy region for both molecules are tabulated in table 2.

4. Conclusions

SXR absorption measurements are presented for carbon dioxide and methane photoionized plasmas. Our results indicate the presence of neutral molecules, atoms, molecular and atomic ions at high SXR intensities. The aforementioned species result from fragmentation of the parent molecules (CH_4 , CO_2) when irradiated by the SXRs. Identification of the corresponding transitions, revealed the creation of L-shell holes in singly charged carbon ions. To our knowledge, SXR absorption studies in molecular plasmas using this LPP scheme have not been reported in the literature before.

Acknowledgments

The work is supported by the Education, Audio-visual and Culture Executive Agency (EACEA) Erasmus Mundus Joint Doctorate Programme EXTATIC, Project No. 2013 0033 and Science Foundation Ireland Grant No. 16/RI/3696. Work associated with EU H2020 COST Action No. CA17126 (TUMIEE). This work was partially supported by the

National Science Centre, Poland, grant agreement no. UMO-2016/23/B/ST7/00949.

ORCID iDs

Lazaros Varvarezos  <https://orcid.org/0000-0002-6781-6616>

Hu Lu  <https://orcid.org/0000-0001-5481-5078>

John T Costello  <https://orcid.org/0000-0003-4677-9999>

Przemyslaw Wachulak  <https://orcid.org/0000-0001-9853-7946>

References

- [1] Takahashi E J, Kanai T, Ishikawa K L, Nabekawa Y and Midorikawa K 2008 *Phys. Rev. Lett.* **101** 253901
- [2] Spielmann C, Burnett N H, Sartania S, Koppitsch R, Schnürer M, Kan C, Lenzner M, Wobrauschek P and Krausz F 1997 *Science* **278** 661–4
- [3] Fiedorowicz H, Bartnik A, Jarocki R, Rakowski R and Szczurek M 2000 *Appl. Phys. B: Lasers Opt.* **70** 305–8
- [4] Bartnik A, Wachulak P, Fiedorowicz H, Jarocki R, Kostecki J and Szczurek M 2013 *Radiat. Phys. Chem.* **93** 9–13
- [5] Saber I, Bartnik A, Wachulak P, Skrzeczanowski W, Jarocki R and Fiedorowicz H 2018 *Springer Proc. Phys.* **202** 203–11
- [6] Bartnik A, Wachulak P, Fiedorowicz H, Fok T, Jarocki R and Szczurek M 2013 *Phys. Plasmas* **20** 1–7
- [7] Bartnik A, Wachulak P, Fiedorowicz H and Skrzeczanowski W 2016 *Phys. Plasmas* **23** 043512
- [8] Bartnik A, Skrzeczanowski W, Fiedorowicz H, Wachulak P and Fok T 2018 *Laser Part. Beams* **36** 76–83
- [9] Bartnik A, Wachulak P, Fiedorowicz H, Skrzeczanowski W, Jarocki R, Fok T and Wegrzyński Ł 2016 *J. Instrum.* **11** C03009
- [10] Bartnik A, Fiedorowicz H, Wachulak P and Fok T 2018 *Laser Part. Beams* **36** 286–92
- [11] Larsson M, Geppert W D and Nyman G 2012 *Rep. Prog. Phys.* **75** 066901
- [12] West J B 2001 *J. Phys. B: At. Mol. Phys.* **34** R45–91
- [13] Lyon I C, Peart B, West J B and Dolder K 1986 *J. Phys. B: At. Mol. Phys.* **19** 4137–47
- [14] Lyon I C, Peart B, Dolder K and West J B 1987 *J. Phys. B: At. Mol. Phys.* **20** 1471–7
- [15] Koizumi T, Itoh Y, Sano M, Kimura M, Kojima T M, Kravis S, Matsumoto A, Oura M, Sekioka T and Awaya Y 1995 *J. Phys. B: At. Mol. Phys.* **28** 609–16
- [16] Covington A M et al 2002 *Phys. Rev. A* **66** 062710
- [17] Gharaibeh M F et al 2011 *J. Phys. B: At. Mol. Phys.* **44** 175208
- [18] Schippers S et al 2019 *X-Ray Spectrom.* **49** 11–20
- [19] Kennedy E, Costello J, Mosnier J P and van Kampen P 2004 *Radiat. Phys. Chem.* **70** 291–321
- [20] Carillon A, Jaegle P and Dhez P 1970 *Phys. Rev. Lett.* **25** 140–3
- [21] Balmer J, Lewis C L S, Corbett R E, Robertson E, Saadat S, O'Neill D, Kilkenny J D, Back C A and Lee R W 1989 *Phys. Rev. A* **40** 330–40
- [22] D'Arcy R, Costello J T, McGuinness C and O'Sullivan G 1999 *J. Phys. B: At. Mol. Phys.* **32** 4859–76
- [23] Adamovich I et al 2017 *J. Phys. D: Appl. Phys.* **50** 323001
- [24] Remington B A, Drake R P and Ryutov D D 2006 *Rev. Mod. Phys.* **78** 755–807

- [25] Jannitti E, Nicolosi P and Tondello G 1990 *Phys. Scr.* **41** 458–63
- [26] Schlachter A S *et al* 2004 *J. Phys. B: At. Mol. Phys.* **37** L103–9
- [27] Rakowski R, Bartnik A, Fiedorowicz H, De Gaufridy De Dortan F, Jarocki R, Kostecki J, Mikołajczyk J, Ryc L, Szczurek M and Wachulak P 2010 *Appl. Phys. B: Lasers Opt.* **101** 773–89
- [28] Kita T, Harada T, Nakano N and Kuroda H 1983 *Appl. Opt.* **22** 512–3
- [29] Harada T and Kita T 1980 *Appl. Opt.* **19** 3987–93
- [30] Wachulak P W *et al* 2010 *Appl. Phys. B: Lasers Opt.* **100** 461–9
- [31] Wachulak P, Duda M, Fok T, Bartnik A, Wang Z, Huang Q, Sarzyński A, Jancarek A and Fiedorowicz H 2018 *Materials* **11** 1303
- [32] Kelly R L 1988 *J. Phys. Chem. Ref. Data* **16** 1–649
- [33] Hitchcock A and Mancini D 1994 *J. Electron. Spectrosc. Relat. Phenom.* **67** 7
- [34] Sham T K, Yang B X, Kirz J and Tse J S 1989 *Phys. Rev. A* **40** 652–69
- [35] Bozek J D, Saito N and Suzuki I H 1995 *Phys. Rev. A* **51** 4563–74
- [36] Ma Y, Chen C T, Meigs G, Randall K and Sette F 1991 *Phys. Rev. A* **44** 1848–58
- [37] Urquhart S G and Gillies R 2005 *J. Phys. Chem. A* **109** 2151–9
- [38] Wight G and Brion C 1974 *J. Electron. Spectrosc. Relat. Phenom.* **4** 335–45
- [39] Ueda K, Okunishi M, Chiba H, Shimizu Y, Ohmori K, Sato Y, Shigemasa E and Kosugi N 1995 *Chem. Phys. Lett.* **236** 311–7
- [40] Kivimäki A, Neeb M, Kempgens B, Köppe H M and Bradshaw A M 1996 *J. Phys. B: At. Mol. Phys.* **29** 2701–9
- [41] Ekström U, Carravetta V, Alagia M, Lavolle M, Richter R, Bolcato C and Stranges S 2008 *J. Chem. Phys.* **128** 044302
- [42] Dujardin G, Winkoun D and Leach S 1985 *Phys. Rev. A* **31** 3027–38
- [43] Berg L E, Karawajczyk A and Stromholm C 1994 *J. Phys. B: At. Mol. Phys.* **27** 2971–80
- [44] Hatherly P A, Codling K, Stankiewicz M and Roper M 1995 *J. Phys. B: At. Mol. Phys.* **28** 3249–60
- [45] Pešić Z D, Rolles D, Bilodeau R C, Dimitriu I and Berrah N 2008 *Phys. Rev. A* **78** 051401
- [46] Cowan R D 1981 *The Theory of Atomic Structure and Spectra* (Berkeley, CA: University of California Press)
- [47] Kramida A 2019 *Atoms* **7** 64